

RSC Advances



This is an *Accepted Manuscript*, which has been through the Royal Society of Chemistry peer review process and has been accepted for publication.

Accepted Manuscripts are published online shortly after acceptance, before technical editing, formatting and proof reading. Using this free service, authors can make their results available to the community, in citable form, before we publish the edited article. This *Accepted Manuscript* will be replaced by the edited, formatted and paginated article as soon as this is available.

You can find more information about *Accepted Manuscripts* in the [Information for Authors](#).

Please note that technical editing may introduce minor changes to the text and/or graphics, which may alter content. The journal's standard [Terms & Conditions](#) and the [Ethical guidelines](#) still apply. In no event shall the Royal Society of Chemistry be held responsible for any errors or omissions in this *Accepted Manuscript* or any consequences arising from the use of any information it contains.

ARTICLE

A facile CO₂ switchable nanocomposite with reversible transition from sol to self-healable hydrogel

Cite this: DOI: 10.1039/x0xx00000x

Lei Zhang,^{a,b} Jiasheng Qian,^b Yujiao Fan,^a Wei Feng,^a Zhen Tao,^a and Haiyang Yang^{*a}Received 00th January 2012,
Accepted 00th January 2012

DOI: 10.1039/x0xx00000x

www.rsc.org/

Abstract: In this paper, we report a CO₂/N₂-switchable sol to gel transition system based on a triblock copolymer of dimethylaminoethyl methacrylate (DMAEMA) and ethylene oxide (EO), with a measured composition DMAEMA₆-EO₁₀₉-DMAEMA₆, in aqueous nanoclay dispersions. Laponite is exfoliated and stabilized by Pluronic F127. The aqueous mixture exhibits a strong response to CO₂, changing from a low viscous sol to a self-healable gel. In the presence of CO₂, the PDMAEMA blocks are protonated and the positive charged triblock copolymer bridge the negative charged nanoclays, formation of a physical network. As a consequence, a sol to gel transition is observed at the macro level. Upon removal of CO₂ through bubbling with N₂, a corresponding gel to sol transition occurs due to the deconstruction of the physical network, which is a result of the departure of the deprotonated PDMAEMA blocks from the nanoclays. This sol to gel transition is fully reversible. Furthermore, the formed gel possesses excellent self-healing ability, meaning that this hydrogel is capable of autonomous healing upon damage. Thus, we believe the fundamentals of the present CO₂-responsive smart hydrogel may hold promise for a wide range of areas, such as intelligent delivery systems and smart biomaterial fields, or a potential CO₂ plugging agent for enhanced oil recovery (EOR) performed by CO₂ flooding.

Introduction

Valorizing the use of CO₂ has been extensively investigated for its nontoxicity, abundance and low cost. CO₂-responsive polymers provide the advantage to use CO₂ as a “green” trigger as well as to capture CO₂ directly from air¹. Generally, CO₂-responsive groups are classified as amidine, amine and carboxyl groups.²⁻⁵ Amidine is a type of gas-switchable molecule that was pioneered by Jessop et al.^{6, 7} They also investigated CO₂-switchable hydrophilicity of solvents for the first time which were used to extract low-polarity organic products.⁸ So far, various CO₂-responsive polymers have been reported for widespread potential applications. Zhao et al discovered that poly(N,N-dimethylaminoethylmethacrylate) (PDMAEMA) in water could react with CO₂ through the side amine groups and designed a general strategy that makes the making of polymers with a CO₂-switchable lower critical solution temperature easily accessible.⁹ The reaction of

DMAEMA units with CO₂ is a facile strategy to fabricate CO₂-responsive systems without demanding synthesis and hydrolyzation compared to incorporating the amidine functionality into a polymer structure.^{10, 11}

LaponiteXLG [Na_{0.7} (Si₈Mg_{5.5}Li_{0.3})O₂₀(OH)₄], a synthetic layered smectite silicate clay with an average diameter of 25 nm and thickness of 1 nm, possesses a permanent negative surface charge arising from isomorphous substitutions in the crystal structure and a pH dependent edge charge from unsatisfied valences in the disrupted crystal lattice ions.^{12, 13} It has attracted considerable interest as a physical crosslinkage incorporated into the nanocomposite hydrogels to pursue superior mechanical properties such as high strength and toughness.¹⁴⁻¹⁷ However, to our knowledge, few studies have focused on the stimulus-responsiveness of the nanocomposite system, especially with CO₂ as a simple and “green” trigger, which we believe can open new opportunities for the nanocomposite systems.

In this paper, we present a new reversible sol to gel transition based on a nanocomposite triblock copolymer system, which was fabricated through mixing the synthetic triblock copolymer, PDMAEMA₆-PEO₁₀₉-PDMAEMA₆, into the aqueous nanoclay dispersion. Upon bubbling with CO₂, the liquid mixture was converted to an elastic predominantly gel, which turned back to the initial sol state after N₂ bubbling. This transition is fully reversible. Besides, rheological measurements demonstrated this gel possessed excellent self-healing ability. The damaged gel could be autonomously repairable without extra healable additives. To date, CO₂ responsiveness of a nanocomposite system has not been reported before. Here, we proposed a possible mechanism for the interaction between the triblock copolymer and the nanoclays, which was demonstrated by ¹HNMR, conductivity, rheological measurements and scanning electron microscope (SEM). These properties with corresponding fundamentals make such CO₂ responsive materials potential candidates for CO₂ plugging agent in enhanced oil recovery or to be used in intelligent delivery systems and smart biomaterial fields.

Experiments Part

Materials

Laponite XLG was purchased from Rockwood Additives Ltd. Pluronic F127 (PF127) was from Sigma Aldrich. PEO (4000) was received from BASF, with a measured molecular weight 4880. PDMAEMA₆-b-PEO₁₀₉-b-PDMAEMA₆ was synthesized according to previous methods.^{18, 19}

Sample preparation

First, appropriate amounts of laponite nanoparticles were added into water under vigorous stirring. Then ultrasonic dispersion was continued for 1h at 40kHz to completely decentralize the nanoparticles. Quantitative PF127 was added to the aqueous dispersion, and the mixture was stirred for another 1h. At last, the triblock copolymer was added into the mixture to obtain a homogeneous solution. To investigate the influence of the copolymer on the system, various contents of the copolymer in nanoclay dispersions were prepared. If not otherwise indicated, the weight percent was set to 3% for laponite and 3.6% for PF127. Various solutions with different polymer concentration (C_p) were prepared in order to make a comparison.

For the gelation experiment, CO₂ was bubbled into the final solution for 5 min. Then the sample was equilibrated in a sealed vial for 24h before subsequent tests. The formed gel was converted to the sol state via stirring under a nitrogen atmosphere.

Rheological Studies

Steady and dynamic rheological measurements were performed on an ARG2 stress controlled rheometer (TA AR-G2) at 25 °C on a cone-and-plate geometry (diameter 40mm, cone angle 4°). Frequency sweep was conducted within a linear viscoelastic regime, which was determined by the stress-sweep test.

Results and Discussion

CO₂ responsiveness of PDMAEMA₆-b-PEO₁₀₉-b-PDMAEMA₆

CO₂ responsiveness was successfully demonstrated by ¹HNMR spectra and conductivity measurement. As is shown in Fig 2a, the tertiary amine groups in PDMAEMA blocks could be protonated by the reaction with CO₂ and deprotonated upon N₂ addition. Upon bubbling CO₂ at room temperature, the reaction of PDMAEMA with CO₂ results in the protonation of the amine groups by carbonic acid, which leads to the formation of charged and more water-soluble ammonium

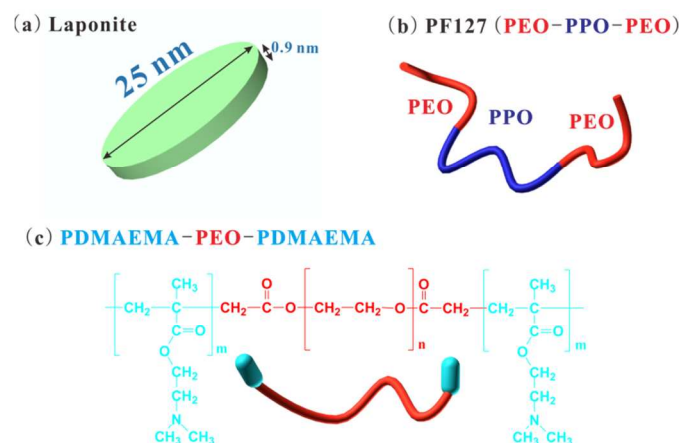


Figure 1. The key components, (a) Laponite nanosheet, (b) PF127, and (c) the synthetic copolymer PDMAEMA₆-PEO₁₀₉-PDMAEMA₆.

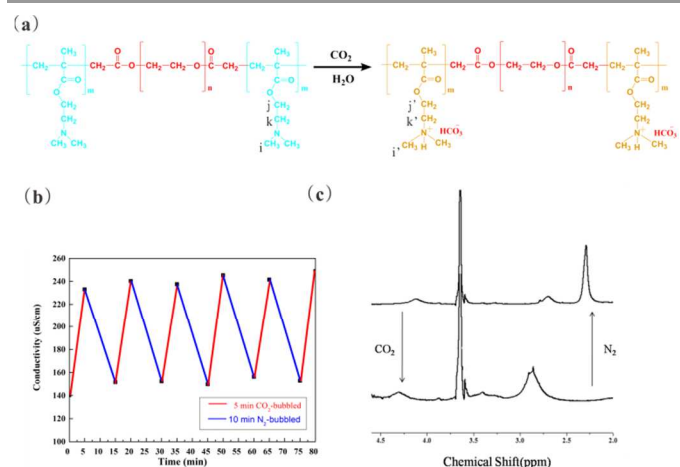


Figure 2 a. Transition of tertiary amine groups to the protonated state in the presence of CO₂; b. Reversible change in the conductivity upon alternating bubbling with CO₂ (5min) and N₂ (10min); c ¹HNMR spectra of the copolymer in D₂O upon alternating bubbling with CO₂ and N₂.

bicarbonates. As an evidence of this, ¹HNMR spectra of the copolymer dissolved in D₂O before CO₂ and after CO₂ bubbling through the solution were recorded. A downfield shift of the resonance peaks was observed (Fig 2c), indicating the formation of bicarbonate salts of protonated amine groups. Meanwhile, the conductivity showed an obvious enhancement from 140uS/cm to 230uS/cm (Fig 2b). After bubbling N₂ for

10min, PDMAEMA segments were deprotonated, which was confirmed by the upfield shift to the original value from $^1\text{H NMR}$. Correspondingly, the conductivity dropped to a minimum value close to the original one, too. The following 4 cycles presented a similar phenomenon and this aqueous solution exhibited the same conductivity variation, implying that the protonation and deprotonation of the synthetic PDMAEMA blocks were fully invertible.

CO₂-induced gelation

Previous studies demonstrated the adsorption behavior of PF127 on the nanoclays.²⁰ The hydrophobic PPO blocks preferred to locate at the surface, largely excluding the PEO block, which formed freely dangling tails. Thus the steric hindrance of PEO block enabled the exfoliation of nanoclays from each other. After dissolution of the triblock copolymer, the final solution maintained a homogeneous state except an ignorable increase of the viscosity appeared (Fig 3a). When subjected to CO₂ bubbling, the low-viscous sol changed to a

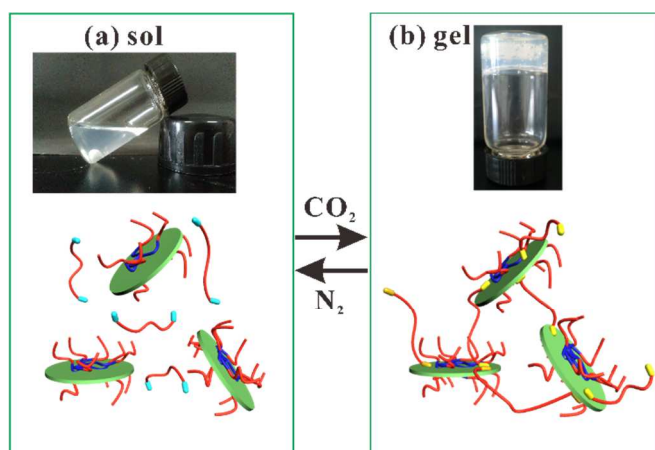


Figure 3. CO₂-induced gelation of the triblock copolymer in aqueous clay dispersion. The system is a low-viscous fluid (a), upon CO₂ bubbling, it is converted into a viscoelastic gel (b); after N₂ passing through, the gel turns back to the initial sol state (a).

gel structure, which was slightly viscoelastic and could hold its own weight in the inverted vial (Fig 3b). The drastic enhancement of viscosity can also be observed from the steady shear measurements (Fig 4), the viscosity of the initial sol state enhanced almost 5 orders after bubbling with CO₂, accompanied by strong shear-thinning phenomenon compared to the original Newtonian fluid behavior. The dramatic change of viscosity indicates the formation of strong electrostatic interaction between the protonated PDMAEMA blocks and the exfoliated nanoclays. Figure 5 depicts the frequency sweep of the formed gel containing different amounts of the copolymer. The storage modulus G' and the loss modulus G'' were measured as a function of frequency within the linear range. For all samples, the G' values had a substantial elastic response and were always larger than the G'' values over the entire range of frequencies ($\tan \delta$ values were much less than 1, Fig 5b), indicative of a predominantly elastic network rather than a viscous sol state after CO₂ bubbling. Further, this gel-like behavior

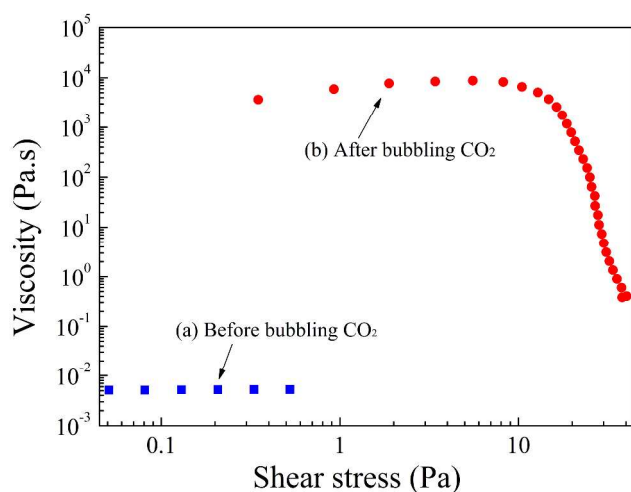


Figure 4 Steady-shear rheology before and after CO₂ bubbling at 25 °C ($C_p=8\text{mg/mL}$).

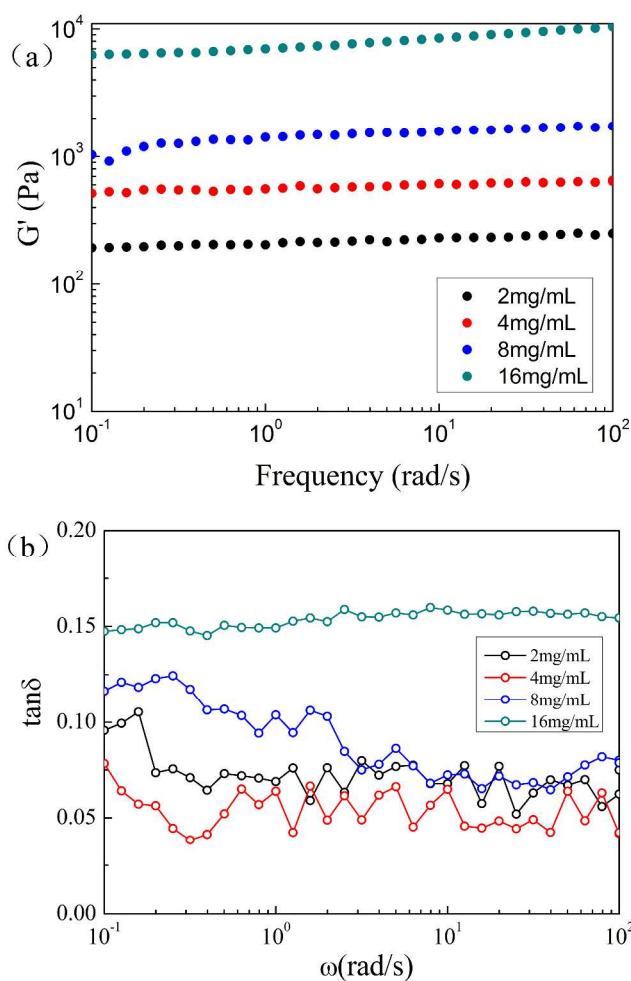


Figure 5 Frequency sweep of the CO₂-induced gel with various contents of the copolymer (C_p) at 25 °C.

manifests that the polymer chains could bridge the clay platelets due to the protonation of the PDMAEMA blocks. The

slight frequency dependence, which was observed frequently in previous studies, was mainly attributed to the relative weak physical interaction of the present networks compared to those strong elastic materials²¹⁻²³. As can be seen, the G' value showed an obvious increment with increase the concentration of the triblock copolymer from 2mg/mL to 16mg/mL (Fig 5a), implying that more crosslinkages were constructed at a higher polymer concentration. It is reasonable that additional crosslink points formed at a higher polymer concentration in the presence of CO₂ compared to a relative lower one, due to a larger degree of protonation of the PDMAEMA blocks.

To gain better insight into the effect of polymer concentration on the nanocomposite system, the phase angle δ , another way of quantifying the gel strength, was measured given by the relation $\tan \delta = G''/G'$ (Fig 5b). The quantity of $\tan \delta$ represents the ratio of dissipated energy to stored energy during one deformation cycle. The lower the value of δ , the more elastic the material is. Generally, a $\tan \delta$ value of >0.1 accompanied by its relatively low frequency dependence is believed to be the typical feature of a so-called weak gel. When compared with the lower polymer concentration systems, the one at 16mg/mL displayed a larger $\tan \delta$ (around 0.15), suggesting that a larger increment of the G'' value occurs when G' increased at the same time. This evidence clearly points to the formation of a more viscous hydrogel structure (also a weak gel) at an overlarge polymer concentration, in contrast to the relative more elastic ones formed at lower polymer concentrations.

The information contained can be conveyed more visualized. Mechanism of the CO₂-switchable ability has been illustrated via the schematic in Fig 3. Before CO₂ bubbling, the nanocomposite system exhibited a liquid-like sol state and the triblock copolymer keep a homogeneously dispersive state at a macro level, without protonation of the PDMAEMA blocks. Upon CO₂ bubbling, the PDMAEMA blocks were protonated and attracted by the negative charged surface of the exfoliated nanoclays, which served as physical crosslinkages, thus formation of the gel network.

Another interesting discovery is that, at a fixed concentration of nanoclay (e.g. 3wt%), an overlarge concentration of the copolymer would compromise the strength of the viscoelastic gel instead. A possible reason is that superabundant positive charged polymer chains may hinder the adsorption process onto the surface of the clay platelets due to excessive repulsive forces between the molecular chains, thus results in the decrease of the strength of the gel.

As is known, in the aqueous solution of nanoclay without dispersants, the clay platelets tend to adopt a house-of-cards type conformation.²⁴ Here, we make a comparison between this control sample and the present nanocomposite/polymer system. The morphologies difference between the pure laponite gel (the control sample) and the CO₂-induced gel was revealed via SEM images (Fig.6). Morphology of the former shows regular laminar structures with smooth surfaces belong to the nanoclays. In contrast, the latter possessed a irregular morphology, which was mainly attributed to the adsorption of the polymer chains to the nanoclay surface after protonation of the PDMAEMA

blocks upon CO₂ bubbling. The structure difference was further investigated via rheological measurements.

As the G' plateau indicates elastic behavior, and the weak frequency dependence of the control sample implies that it does not relax, that is, it has an infinite relaxation time or at least much longer than the nanocomposite system, which exhibited an relative more obvious frequency dependence over the total range.

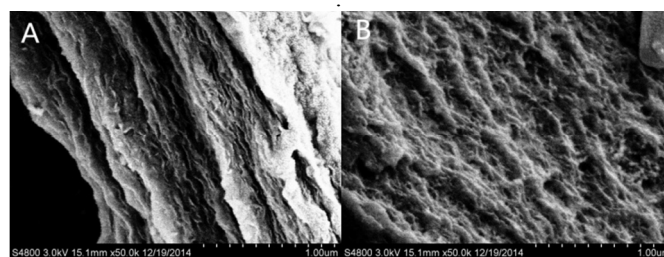


Figure 6 SEM images of (A) pure laponite gel and (B) gel mixture, $C_p=16\text{mg/mL}$. The pure laponite gel has a regular laminar morphology where all layers have similar size. The gel mixture has a relative random morphology: there are some aggregates which connect each other and these aggregates are dispersed irregularly.

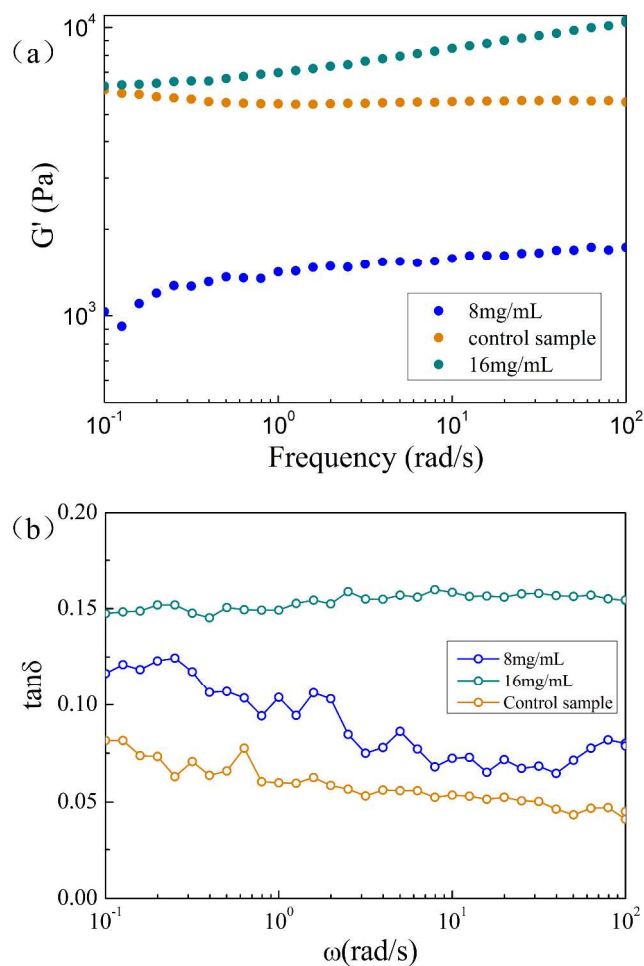


Figure 7 Frequency sweep of the CO₂-induced gel and a controlled sample (pure nanoclay gel) at 25 °C.

The much smaller value of $\tan \delta$ corresponding to the control sample (Fig. 7b) demonstrated that the network of the nanoclay gel possessed a predominantly elastic nature in contrast to the nanocomposite one. One should note the completely different mechanisms for the two gel systems. Previous studies have confirmed that the nanoclay gel network was constructed through electrostatic attraction from the permanent negative surface charge via the positive edge charge of the clay platelets, formation of a house-of-card structure without delamination of the platelets. However, this is not the case for the nanocomposite system, because the laponite nanoparticles were exfoliated by Pluronic F127 before the following connection through the protonated polymeric chains. Undoubtedly, exfoliated nanoclays offer the opportunity to form more cross-linked points than the conglomerate ones as long as the polymer concentration is suitable to provide enough protonated PDMAEMA blocks upon CO₂ bubbling. In fact, we found that when the polymer concentration was below a critical value, the G' value was much smaller than the control sample, but instead, when the concentration is above the critical value (e.g. 16mg/mL), the nanocomposite system exhibited a larger G' value over the frequency range. This phenomenon effectively conforms to our discussion, in which introduction of the protonated PDMAEMA into the exfoliated nanoclay dispersion replaced the elastic predominantly house-of-cards structure with a relative more viscoelastic structure.

Reversibility of CO₂-induced gelation

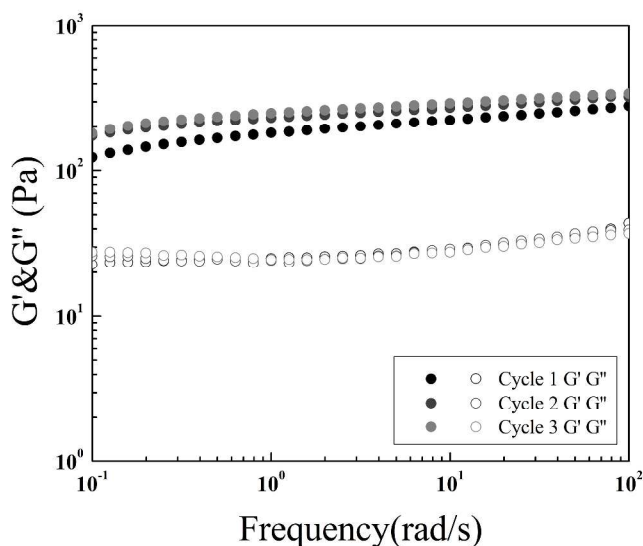


Figure 8 Frequency sweep of the CO₂-induced hydrogel for 3 cycles at 25 °C. (C_p=2mg/mL)

Generally, laponite gels lack the switchable ability in response to external stimuli. Here, we have successfully proved that the nanocomposite sol-to-gel transition was fully reversible upon alternatively passing through CO₂/N₂. Figure 8 shows variation

of the G' and G'' values of the invertible gel during three cycles of CO₂ and N₂ bubbling. Excellent superposition of both G' and G'' curves versus frequency was observed, with G' value for the first cycle possessing a negligible deviation compared to the following two cycles. This finding indicates that both the gel strength and its frequency dependence kept almost consistent after CO₂ bubbling in three cycles. The same G' and G'' values suggested perfect reconstruction of the gel network in the presence of CO₂, while the identical frequency dependence is a symbol of similar viscoelasticity change for the network.

Self-healing study of the CO₂-induced gel

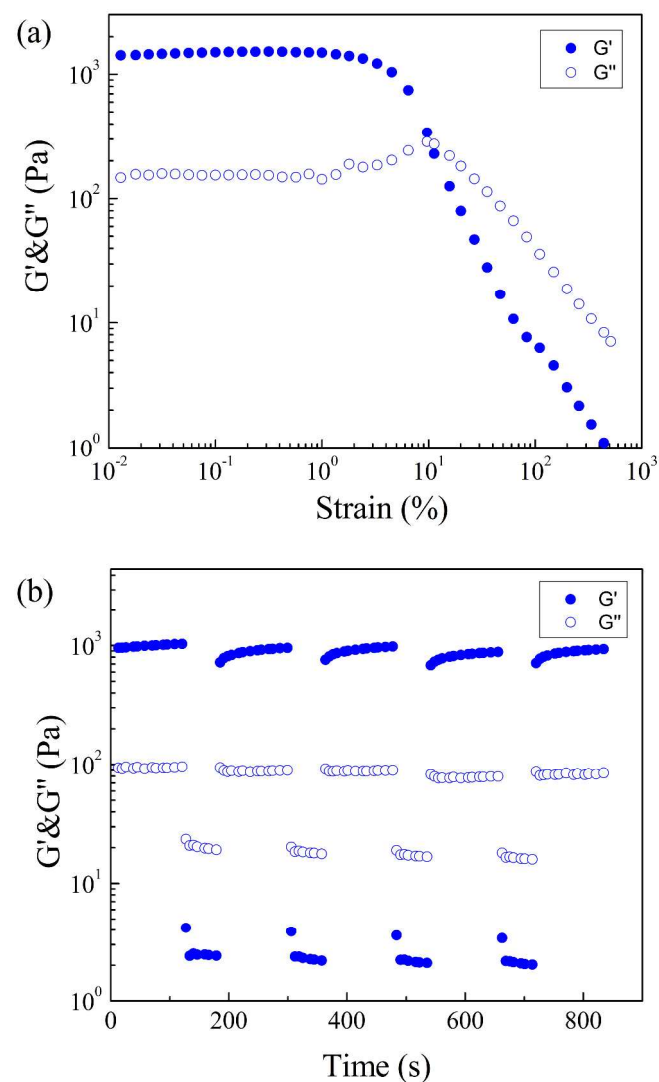


Figure 9 (a) G' and G'' of the hydrogel (C_p=8mg/mL) as a function of strain at 25 °C. (b) Evolution of G' and G'' with time following two successive pulses of high deformation.

An autonomous self-healable material upon damage would be highly desirable for materials. Here, we considered that the nanocomposite hydrogel in response to CO₂ to show self-healing behaviour.

As shown in Fig. 9a, under small strain, G' was larger than G'' , indicative of an elastic dominated structure and the gel network remained unaffected due to the intact crosslinkages. However, there was a gel to liquid transition point (strain=11%, stress=228.7Pa) denoted as a breakdown of the gel state to a quasi-liquid state above a threshold strain. G'' stayed larger than G' above this critical point, confirming deconstruction of the gel network due to the disassociation of the crosslinkages at high shear strain.

Figure 9b exhibit the rheological behaviour of the gel structure under a strain pulse deformation program, in which the strain increases from 0.1% to 80% at a certain time point and then returns to 0.1% at a certain period ($f=1$ Hz). It can be seen that the G' and G'' values are completely inverted under a high deformation strain (80%), implying that the gel network was thoroughly destroyed to a sol state. After decreasing the amplitude (strain=0.1%), the G' and G'' recovered back to their original values rapidly, indicating the quick reconstruction of the gel network, thus confirming the excellent self-healing capability of the hydrogel. The dynamic crosslinkages from the positively charged PDMAEMA blocks and the negatively charged nanoclays undoubtedly contributes to the fast rebuilding process of the physical hydrogel. This spontaneous self-healing property is a result of the synergetic manner from both nanoclay and the protonated polymic bridges, where CO_2 is critical to the formation of the healable hydrogel from the initial sol state.

Conclusions

We demonstrate herein the first fabrication of a CO_2 -switchable sol to gel transition for the nanocomposite system based on triblock copolymer, PDMAEMA₆-PEO₁₀₉-PDMAEMA₆, and laponite nanoclay dispersion. Reversible protonation/deprotonation of the terminal PDMAEMA blocks upon CO_2 addition and its removal allow the corresponding adsorption/desorption of the polymer chains to the laponite nanoclays, thus formation of the invertible sol to gel transition. The CO_2 triggered hydrogel possesses rapid and efficient self-healing capability at room temperature, without any need for external stimuli. Repeatable fast rebuilding of the crosslinkages after damage is ascribed to the spontaneous electrostatic attraction between protonated PDMAEMA blocks and laponite nanoclays. One should note that structure of the polymer should not be limited to the present one, besides, mechanical properties of the formed hydrogel can be further tuned through designing the molecular structure, the dosage of laponite nanoclays and polymer concentration. This facile strategy provides better understanding of smart response nanocomposite hydrogel and self-healing materials for extensive applications such as intelligent delivery systems and smart biomaterial fields, or a potential CO_2 plugging agent for enhanced oil recovery (EOR) performed by CO_2 flooding.

Acknowledgements

This work was supported by the National Natural Science Foundation of China (Grant no.51273189), the National Science and Technology Major Project of the Ministry of Science and Technology of China (2011ZX05010-003), Petro China Innovation Foundation (2012D-5006-0202), and China Postdoctoral Science Foundation funded project (no.2013M531513).

Notes and references

^aCAS Key Laboratory of Soft Matter Chemistry, Department of Polymer Science and Engineering, University of Science and Technology of China, Hefei, Anhui 230026, P. R. China.

^bDepartment of Chemistry and Chemical Engineering, Anhui University, Hefei, 230000, P. R. China.

E-mail: yhy@ustc.edu.cn; Fax: +86-551-3607549; Tel: +86-551-3607549

The authors declare no competing financial interests.

1. D. M. Rudkevich, *Angewandte Chemie International Edition*, 2004, **43**, 558-571.
2. D. Nagai, A. Suzuki, Y. Maki and H. Takeno, *Chemical communications*, 2011, **47**, 8856-8858.
3. P. G. Jessop, S. M. Mercer and D. J. Heldebrant, *Energy & Environmental Science*, 2012, **5**, 7240-7253.
4. S. Lin and P. Theato, *Macromolecular Rapid Communications*, 2013, **34**, 1118-1133.
5. Q. Yan, R. Zhou, C. Fu, H. Zhang, Y. Yin and J. Yuan, *Angewandte Chemie*, 2011, **123**, 5025-5029.
6. P. G. Jessop, D. J. Heldebrant, X. Li, C. A. Eckert and C. L. Liotta, *Nature*, 2005, **436**, 1102-1102.
7. Y. Liu, P. G. Jessop, M. Cunningham, C. A. Eckert and C. L. Liotta, *Science*, 2006, **313**, 958-960.
8. P. G. Jessop, L. Phan, A. Carrier, S. Robinson, C. J. Durr and J. R. Harjani, *Green Chemistry*, 2010, **12**, 809-814.
9. D. Han, X. Tong, O. Boissière and Y. Zhao, *ACS Macro Letters*, 2011, **1**, 57-61.
10. B. Yan, D. Han, O. Boissiere, P. Ayotte and Y. Zhao, *Soft Matter*, 2013, **9**, 2011-2016.
11. Y. Qian, Q. Zhang, X. Qiu and S. Zhu, *Green Chemistry*, 2014, **16**, 4963-4968.
12. Negrete, J.-M. Letoffe, J.-L. Putaux, L. David and E. Bourgeat-Lami, *Langmuir*, 2004, **20**, 1564-1571.
13. J. I. Dawson and R. O. C. Oreffo, *Advanced Materials*, 2013, **25**, 4069-4086.
14. K. Haraguchi and T. Takehisa, *Advanced Materials*, 2002, **14**, 1120-1124.
15. J. Ning, G. Li and K. Haraguchi, *Macromolecules*, 2013, **46**, 5317-5328.
16. M. Liu, Y. Ishida, Y. Ebina, T. Sasaki, T. Hikima, M. Takata and T. Aida, *Nature*, 2015, **517**, 68-72.
17. Y. Wu, Z. Zhou, Q. Fan, L. Chen and M. Zhu, *Journal of Materials Chemistry*, 2009, **19**, 7340-7346.
18. R. E. Lamont and W. A. Ducker, *Journal of the American Chemical Society*, 1998, **120**, 7602-7607.
19. Y. Sun, Z. Peng, X. Liu and Z. Tong, *Colloid Polym Sci*, 2010, **288**, 997-1003.
20. A. Nelson and T. Cosgrove, *Langmuir*, 2005, **21**, 9176-9182.
21. C. A. Bonino, J. E. Samorezov, O. Jeon, E. Alsberg and S. A. Khan, *Soft Matter*, 2011, **7**, 11510-11517.
22. Z. Hu and G. Chen, *RSC Advances*, 2013, **3**, 12021-12025.
23. X. Hao, H. Liu, Z. Lu, Y. Xie and H. Yang, *Journal of Materials Chemistry A*, 2013, **1**, 6920-6927.
24. H. Van Olphen, 1977.